Electron Interferometry and EELS

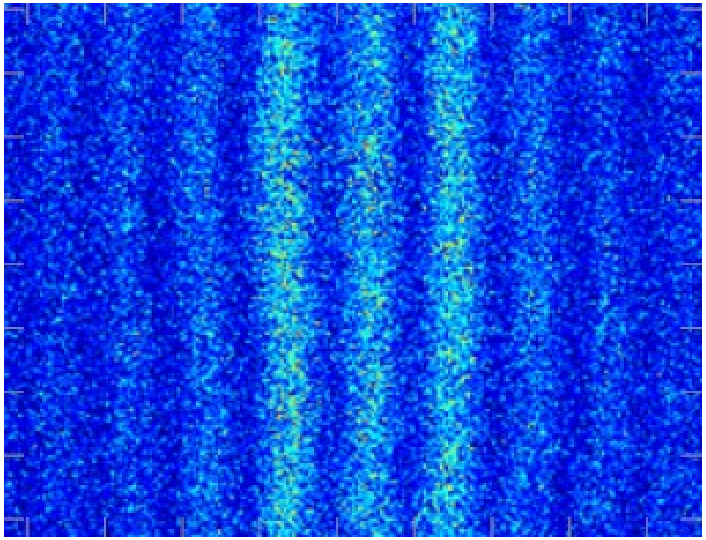

M&M 2026
MICROSCOPY & MICROANALYSIS
August 2-6 • Milwaukee, WI

Dr. David Kordahl

Centenary
COLLEGE OF LOUISIANA

Outline

- Review of electron interferometry experiments
- Examine the logical structure of calculations
- Connect calculations to standard EELS models
- Explore possible “next step” experiments

Fringe Visibility and Decoherence

- Fringe visibility V is a probe of decoherence
- Variation between min and max gives us the visibility

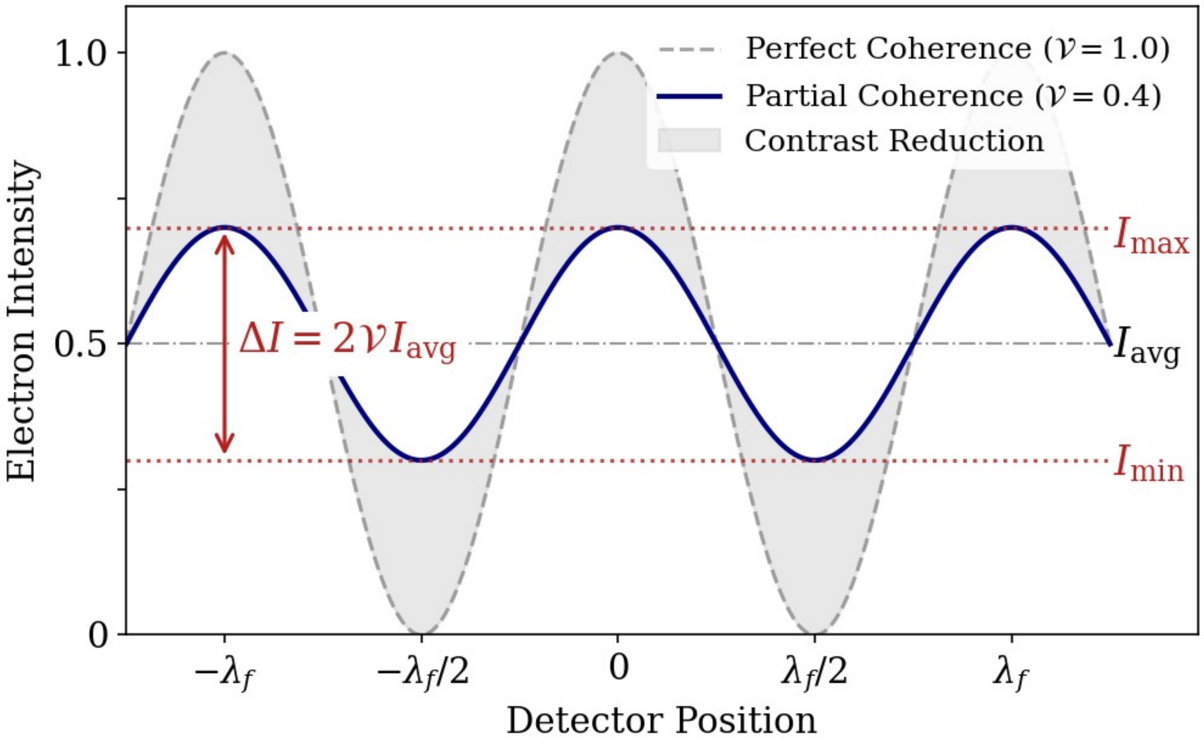

$$\Delta I = I_{\max} - I_{\min} = 2\mathcal{V} I_{\text{avg}}$$

- Limits: $V = 1 \rightarrow$ max contrast
  $V = 0 \rightarrow$ min contrast

Experiments in Fringe Visibility

- Empirically, fringe visibility decreases as the electron
  - Passes nearer to the surface
  - Has farther separated paths

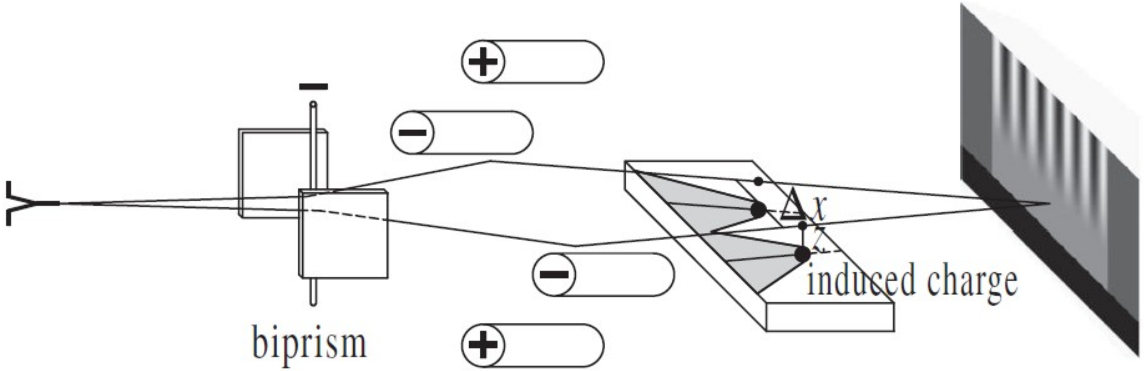

"Measurement of Decoherence of Electron Waves and Visualization of the Quantum-Classical Transition," Peter Sonnentag and Franz Hasselbach, *Physical Review Letters* 98, 200402 (2007)

Experiments in Fringe Visibility

- Empirically, fringe visibility decreases as the electron
  - Passes nearer to the surface
  - Has farther separated paths

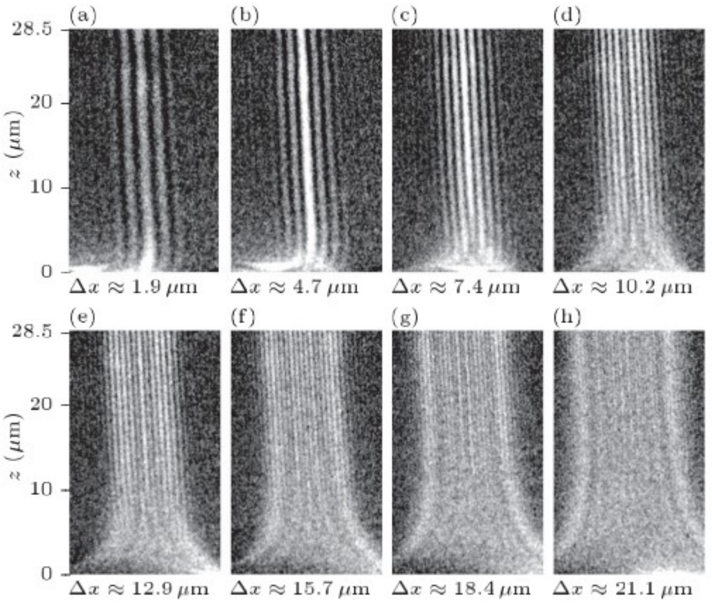

"Measurement of Decoherence of Electron Waves and Visualization of the Quantum-Classical Transition," Peter Sonnentag and Franz Hasselbach, *Physical Review Letters* 98, 200402 (2007)

Experiments in Fringe Visibility

- Empirically, fringe visibility decreases as the electron
  - Passes nearer to the surface
  - Has farther separated paths

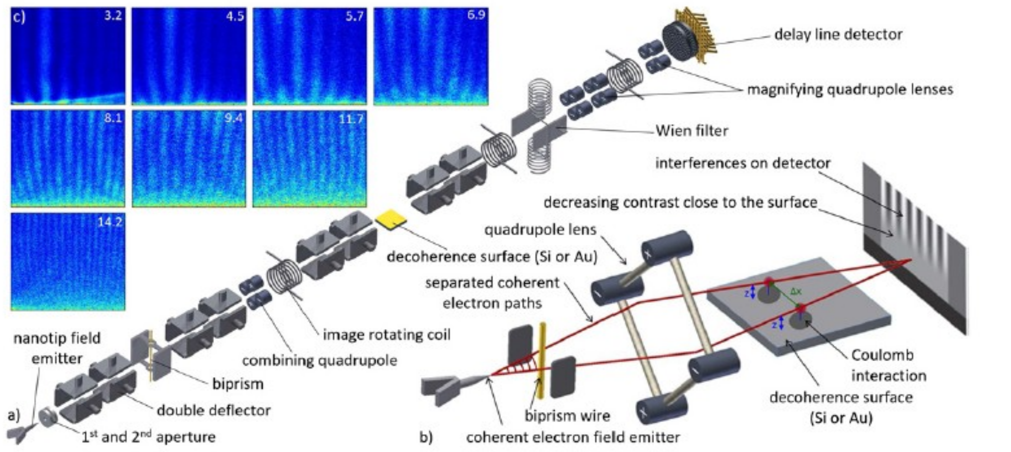

Figure 1. (a) Experimental setup for electron decoherence measurements close to a semiconducting and metallic environment. (b) Sketch of the experiment, where a coherent electron beam is separated and combined by an electrostatic biprism and a quadrupole lens. In the quantum superposition state before interference, the beam passes aloof a semiconducting n-doped silicon or gold surface, interacting with the bulk electron gas. This process causes decoherence which can be observed in a decreasing interference contrast close to the surface. (c) Recorded fringe pattern above the silicon surface (bottom edge of each image) for different beam path separations Δx (value in upper right corner in μm). The top edge is at a height $z = 40$ μm. An increase in signal above the surface up to max 4 μm is visible that is assumed to be due to scattering on waver edge defects.

"Quantum decoherence by Coulomb interaction,"
N. Kerker, R. Röpke, L.M. Steinert, A. Pooch, and A. Stibor,
New Journal of Physics 22 (2020) 0630391

Experiments in Fringe Visibility

- Kerker *et al.* (2020) tested various models of visibility predicted from entanglement of electron and plate

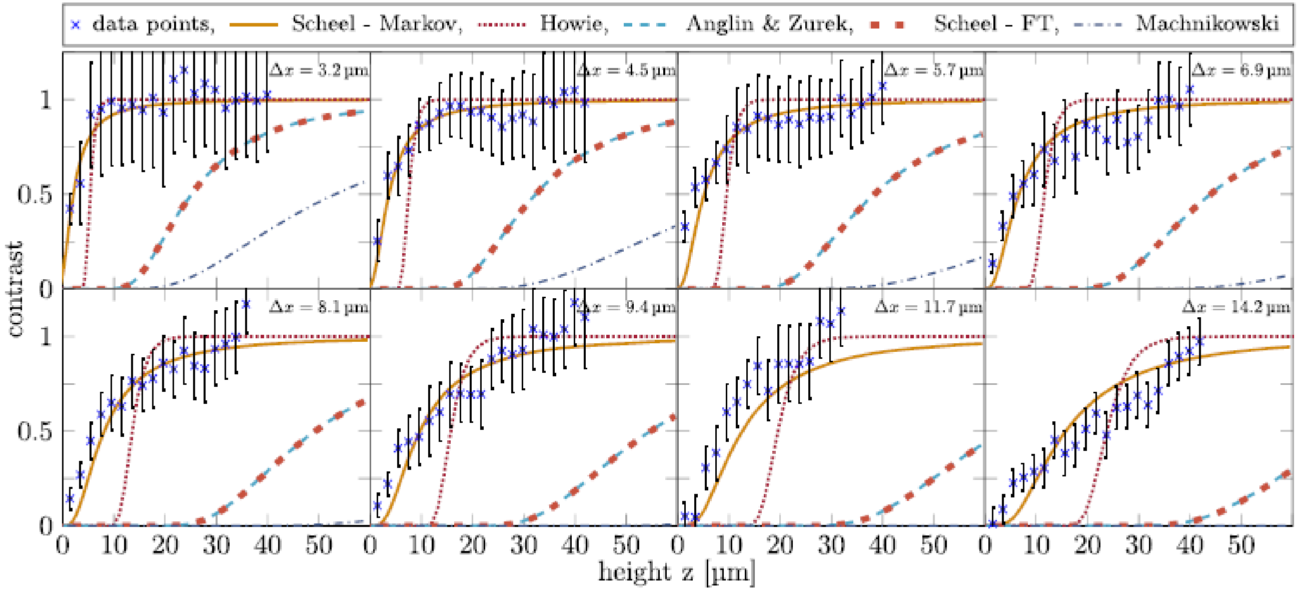

Figure 2. Decoherence of electrons in a superposition state close to a doped silicon surface. The loss of visibility is plotted as a function of distance z to the semiconducting plate for different beam path separations Δx and compared to four current theoretical models [5–8].

Experiments in Fringe Visibility

- Kerker *et al.* (2020) tested various models of visibility predicted from entanglement of electron and plate
- The “Scheel-Markov” theory is basically successful; how does it relate to EELS models?

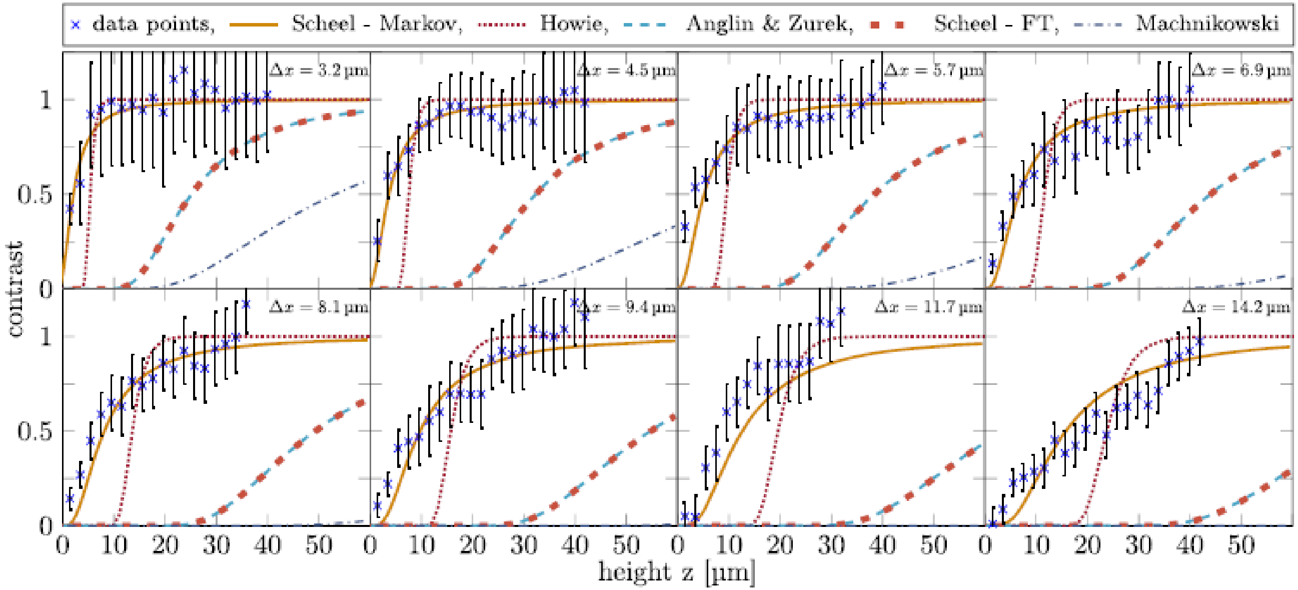

Figure 2. Decoherence of electrons in a superposition state close to a doped silicon surface. The loss of visibility is plotted as a function of distance z to the semiconducting plate for different beam path separations Δx and compared to four current theoretical models [5–8].

Howie's Idea: EELS → Visibility

- Decoherence rate sums EEL spectrum for modes that interact with the different paths differently ($d < \lambda$, or $|k| > \alpha/d$)

"Mechanisms of decoherence in electron microscopy," Archie Howie, *Ultramicroscopy* 111 (2011) 761–767.

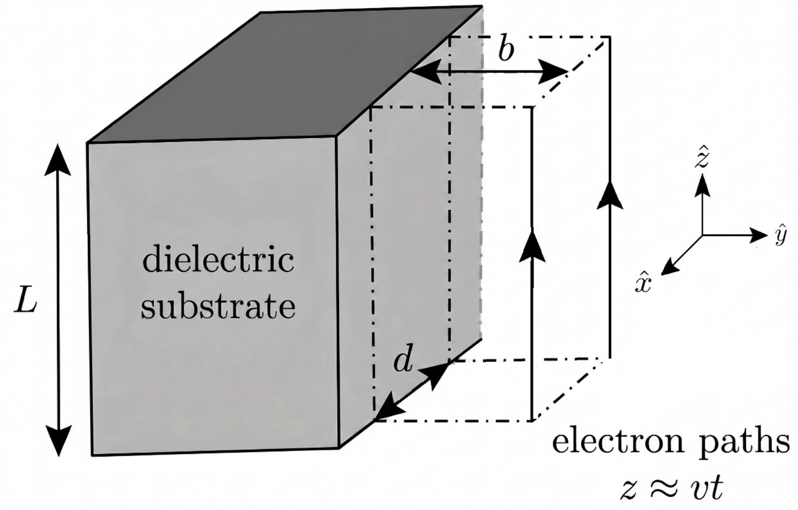

Howie's Idea: EELS → Visibility

- Decoherence rate sums EEL spectrum for modes that interact with the different paths differently
  (d < λ, or |k| > α/d)

$$\gamma(b,d,T) = \int_0^\infty \mathrm{d}\omega \int_{\alpha/d}^\infty \mathrm{d}k_x \, \frac{\mathrm{d}^3 P}{\mathrm{d}\omega\, \mathrm{d}k_x\, \mathrm{d}z} \coth\left(\frac{\hbar\omega}{2k_B T}\right) + \int_0^\infty \mathrm{d}\omega \int_{-\infty}^{-\alpha/d} \mathrm{d}k_x \, \frac{\mathrm{d}^3 P}{\mathrm{d}\omega\, \mathrm{d}k_x\, \mathrm{d}z} \coth\left(\frac{\hbar\omega}{2k_B T}\right)$$

$$\mathcal{V} = \mathrm{e}^{-\gamma(b,d,T)L}$$

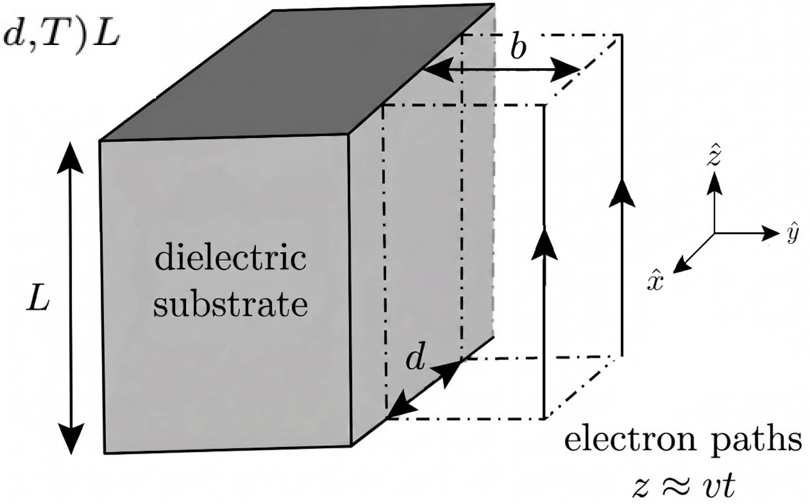

"Mechanisms of decoherence in electron microscopy," Archie Howie, *Ultramicroscopy* 111 (2011) 761–767.

Howie’s Idea:
EELS → Visibility

- Decoherence rate sums EEL spectrum for modes that interact with the different paths differently
  ($d < \lambda$, or $|k| > \alpha/d$)

$$\gamma(b,d,T) = \int_0^\infty \mathrm{d}\omega \int_{\alpha/d}^{\infty} \mathrm{d}k_x \, \frac{\mathrm{d}^3 P}{\mathrm{d}\omega \, \mathrm{d}k_x \, \mathrm{d}z} \coth\left(\frac{\hbar\omega}{2k_B T}\right) + \int_0^\infty \mathrm{d}\omega \int_{-\infty}^{-\alpha/d} \mathrm{d}k_x \, \frac{\mathrm{d}^3 P}{\mathrm{d}\omega \, \mathrm{d}k_x \, \mathrm{d}z} \coth\left(\frac{\hbar\omega}{2k_B T}\right)$$

$$\mathcal{V} = \mathrm{e}^{-\gamma(b,d,T)L}$$

“Mechanisms of decoherence in electron microscopy,” Archie Howie, *Ultramicroscopy* 111 (2011) 761–767.

Right scale…
can we fix
this idea?

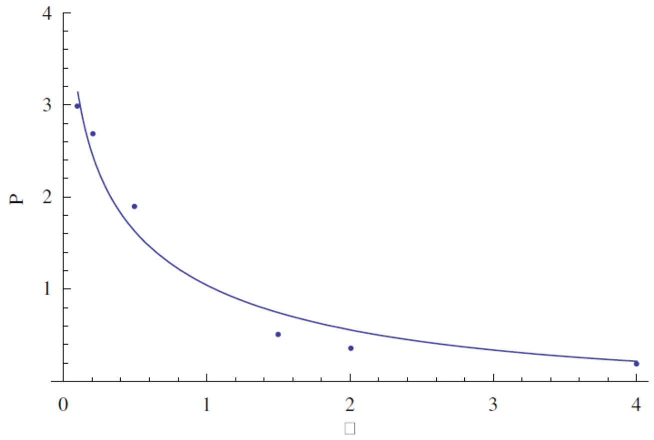

Fig. 4. Comparison between points for $P = -\ln(V)$, where V is the measured fringe visibility in aloof beam electron holography [19] and the theory of Eq. (7) represented by the function $E_1(\eta)$, where $\eta = 4x_0/\Delta y$.

First-Order Interaction Model

- The “which path” information depends on *L*, *d*, and *b*
- Before interaction, assume the substrate is in its ground state, and the electron is in a split-path

$$|\Psi_e\rangle = \frac{1}{\sqrt{2}}\left[\psi_{\rm R}(\mathbf{x}_\perp) + \psi_{\rm L}(\mathbf{x}_\perp)\right]$$

$$|\Psi_i\rangle = |\Psi_e\rangle \otimes |0\rangle$$

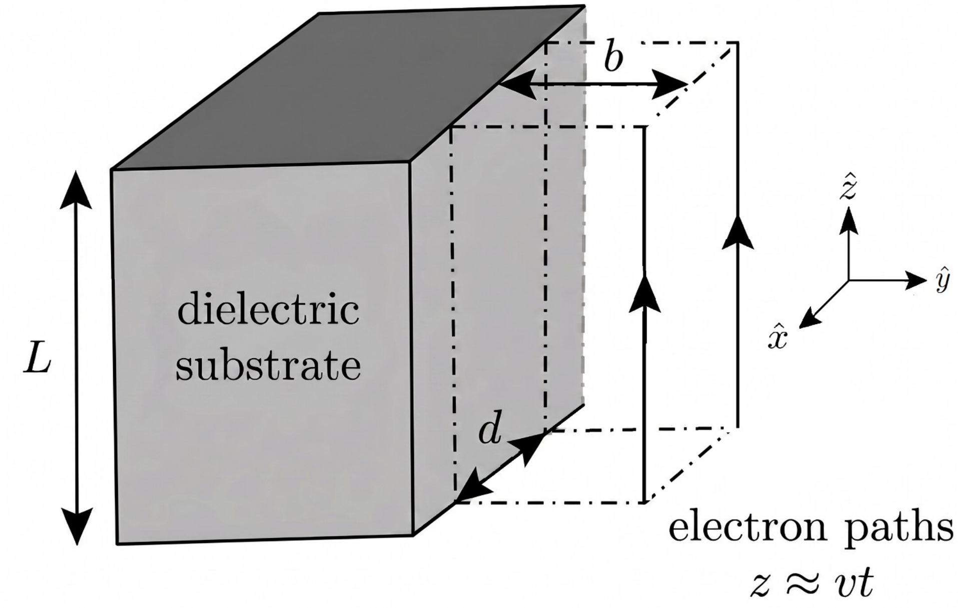

First-Order Interaction Model

- Keeping first-order excitations of surface modes with wavevector **k**, the wavefunction after interaction is

$$|\Psi_f\rangle = \frac{1}{\sqrt{2}}\Bigg[\psi_{\mathrm{R}}(\mathbf{x}_\perp)\left(c_{\mathrm{R}0}\,|0\rangle + \sum_{\mathbf{k}} c_{\mathrm{R}\mathbf{k}}\,|1_{\mathbf{k}}\rangle\right) + \psi_{\mathrm{L}}(\mathbf{x}_\perp)\left(c_{\mathrm{L}0}\,|0\rangle + \sum_{\mathbf{k}} c_{\mathrm{L}\mathbf{k}}\,|1_{\mathbf{k}}\rangle\right)\Bigg]$$

- Afterward, the wave packets are made to overlap, and we sum over surface modes:

$$P_e(\mathbf{x}_\perp) = \sum_{\{n_{\mathbf{k}}\}} \langle\Psi_f|\mathbb{I}_{\mathrm{el}} \otimes |\{n_{\mathbf{k}}\}\rangle\,\langle\{n_{\mathbf{k}}\}|\,|\Psi_f\rangle$$

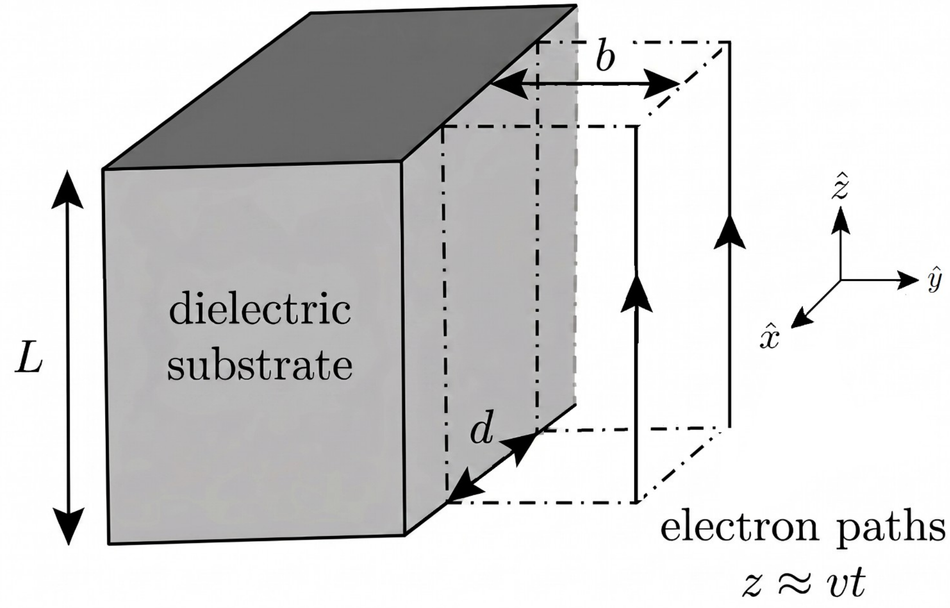

Visibility from First-Order Model

- If paths are equally weighted, we can use symmetry conditions—e.g., $\psi_{\mathrm{R}}(\mathbf{x}_\perp) = \psi_{\mathrm{L}}^*(\mathbf{x}_\perp) = \psi_0(\mathbf{x}_\perp)$
- These conditions allow us to reduce the sum to

$$P_e(\mathbf{x}_\perp) = |\psi_0(\mathbf{x}_\perp)|^2 + \mathrm{Re}\left\{ (\psi_0(\mathbf{x}_\perp))^2 \left[c_{\mathrm{R}0}^* c_{\mathrm{L}0} + \sum_{\mathbf{k}} c_{\mathrm{R}\mathbf{k}}^* c_{\mathrm{L}\mathbf{k}} \right] \right\}$$

to calculate the visibility via scattering coefficients:

$$\mathcal{V} = 1 - \sum_{\mathbf{k}} |c_{\mathbf{k}}|^2 [1 - \cos(k_x d)].$$

Visibility from First-Order Model

- If paths are equally weighted, we can use symmetry conditions—e.g., $\psi_{\mathrm{R}}(\mathbf{x}_\perp) = \psi_{\mathrm{L}}^*(\mathbf{x}_\perp) = \psi_0(\mathbf{x}_\perp)$
- These conditions allow us to reduce the sum to $\mathcal{V}$

$$P_e(\mathbf{x}_\perp) = |\psi_0(\mathbf{x}_\perp)|^2 + \mathrm{Re}\left\{ (\psi_0(\mathbf{x}_\perp))^2 \left[c_{\mathrm{R0}}^* c_{\mathrm{L0}} + \sum_{\mathbf{k}} c_{\mathrm{R}\mathbf{k}}^* c_{\mathrm{L}\mathbf{k}} \right] \right\}$$

to calculate the visibility via scattering coefficients:

$$\mathcal{V} = 1 - \sum_{\mathbf{k}} |c_{\mathbf{k}}|^2 [1 - \cos(k_x d)].$$

Total scattering probability….weighted by path distinguishability

Markov Approximation

- For quantized surface modes, the calculated scattering probability scales with the length *L*

$$|c_{\mathbf{k}}|^2 = L\,\frac{\mathrm{d}P_{\mathbf{k}}}{\mathrm{d}z}$$

$$\mathcal{V}(L) \approx 1 - L\sum_{\mathbf{k}} \frac{\mathrm{d}P_{\mathbf{k}}}{\mathrm{d}z}\left[1-\cos(k_x d)\right]$$

- Now we interpret this as a rate

$$\gamma(b,d) = \sum_{\mathbf{k}} \frac{\mathrm{d}P_{\mathbf{k}}}{\mathrm{d}z}\left[1-\cos(k_x d)\right]$$

$$\frac{\mathrm{d}\mathcal{V}}{\mathrm{d}z} = -\gamma(b,d)\,\mathcal{V}$$

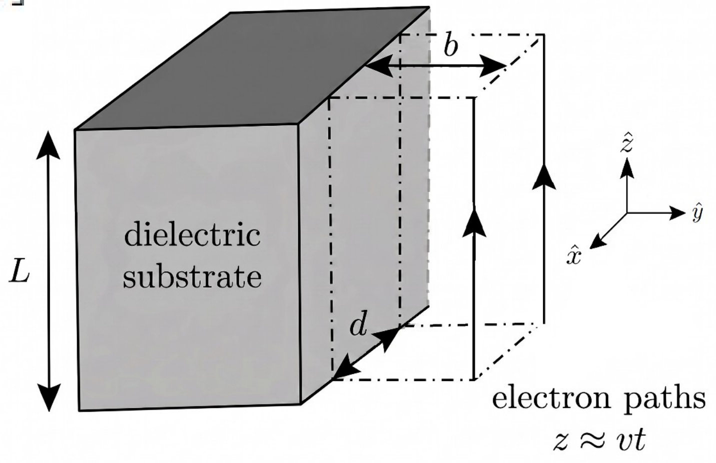

Thermal Weighting

- If we help ourselves to the EELS loss-per-mode-per-unit-length models, we can extend this framework
- If we include thermal occupations of states, we find

$$\gamma(b,d,T) = \int_0^\infty \mathrm{d}\omega \int_{-\infty}^{\infty} \mathrm{d}k_x \, \frac{\mathrm{d}^3 P}{\mathrm{d}\omega \, \mathrm{d}k_x \, \mathrm{d}z} \left[1 - \cos(k_x d)\right] \coth\left(\frac{\hbar\omega}{2k_B T}\right)$$

with the visibility evolving as

$$\mathcal{V} = \exp\left[-\gamma(b,d,T)L\right]$$

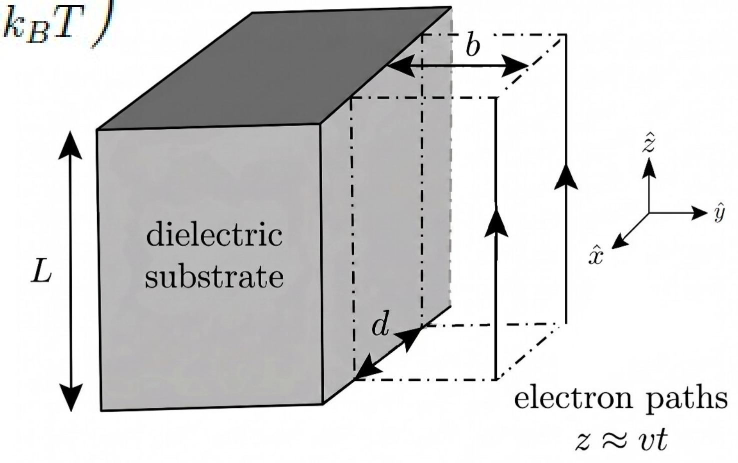

Weighted EELS = “Scheel-Markov”

- If we use electrodynamic EELS loss models in this

$$\gamma(b,d,T) = \int_0^\infty \mathrm{d}\omega \int_{-\infty}^{\infty} \mathrm{d}k_x \, \frac{\mathrm{d}^3 P}{\mathrm{d}\omega\, \mathrm{d}k_x\, \mathrm{d}z} \left[1-\cos(k_x d)\right] \coth\left(\frac{\hbar\omega}{2k_B T}\right)$$

we exactly recover the “Scheel-Markov” model!

S. Scheel and S.Y. Buhmann, “Path decoherence of charged and neutral particles near surfaces,” *Phys. Rev. A,* 030101 (2012)

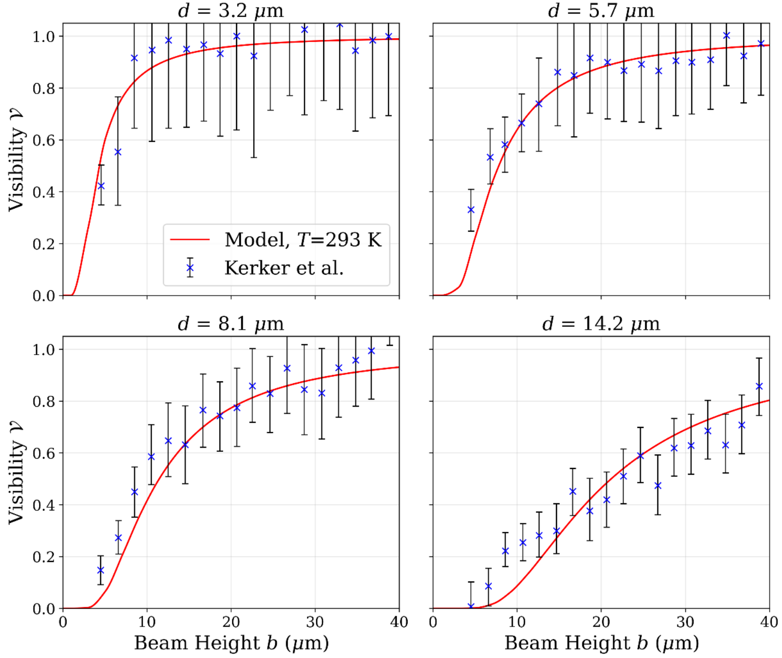

Elements of “Weighted EELS” Model

$$\gamma(b,d,T) = \int_0^\infty \mathrm{d}\omega \int_{-\infty}^{\infty} \mathrm{d}k_x \, \frac{\mathrm{d}^3 P}{\mathrm{d}\omega\, \mathrm{d}k_x\, \mathrm{d}z} \left[1 - \cos(k_x d)\right] \coth\left(\frac{\hbar\omega}{2k_B T}\right)$$

- This decomposition allows us to clearly see where *b*, *d*, and *T* each contribute

$$\mathcal{V} = \exp\left[-\gamma(b,d,T)L\right]$$

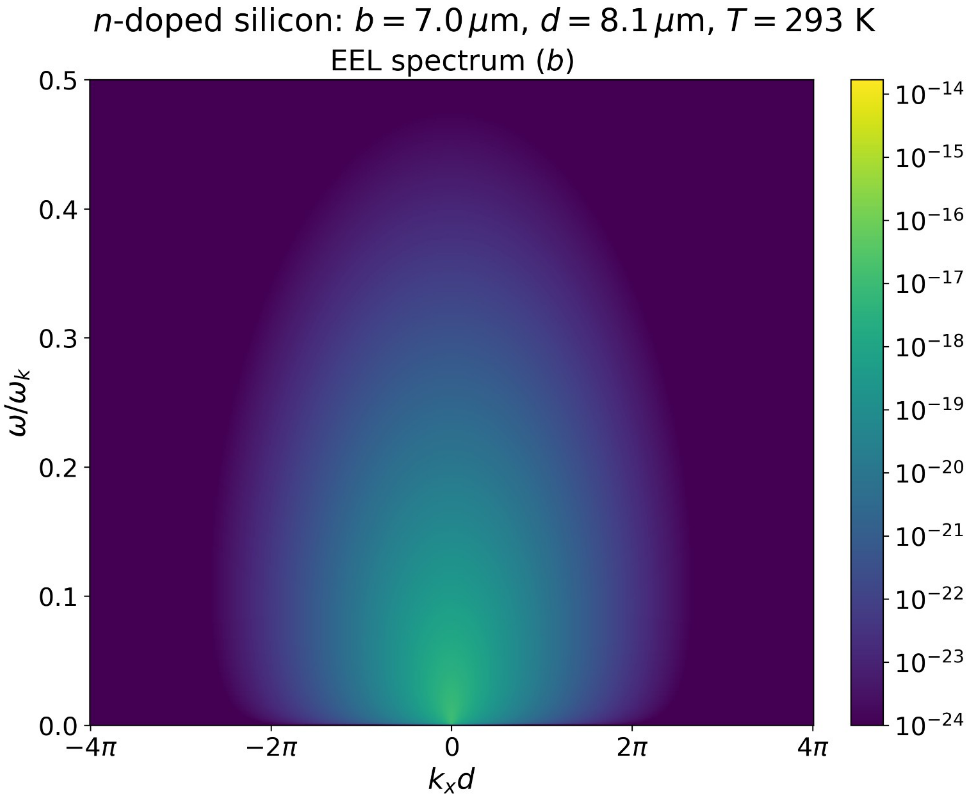

Elements of "Weighted EELS" Model

$$\gamma(b,d,T) = \int_0^\infty \mathrm{d}\omega \int_{-\infty}^\infty \mathrm{d}k_x \frac{\mathrm{d}^3P}{\mathrm{d}\omega\,\mathrm{d}k_x\,\mathrm{d}z}\left[1-\cos(k_x d)\right]\coth\left(\frac{\hbar\omega}{2k_BT}\right)$$

- This decomposition allows us to clearly see where *b*, *d*, and *T* each contribute

$$\mathcal{V} = \exp\left[-\gamma(b,d,T)L\right]$$

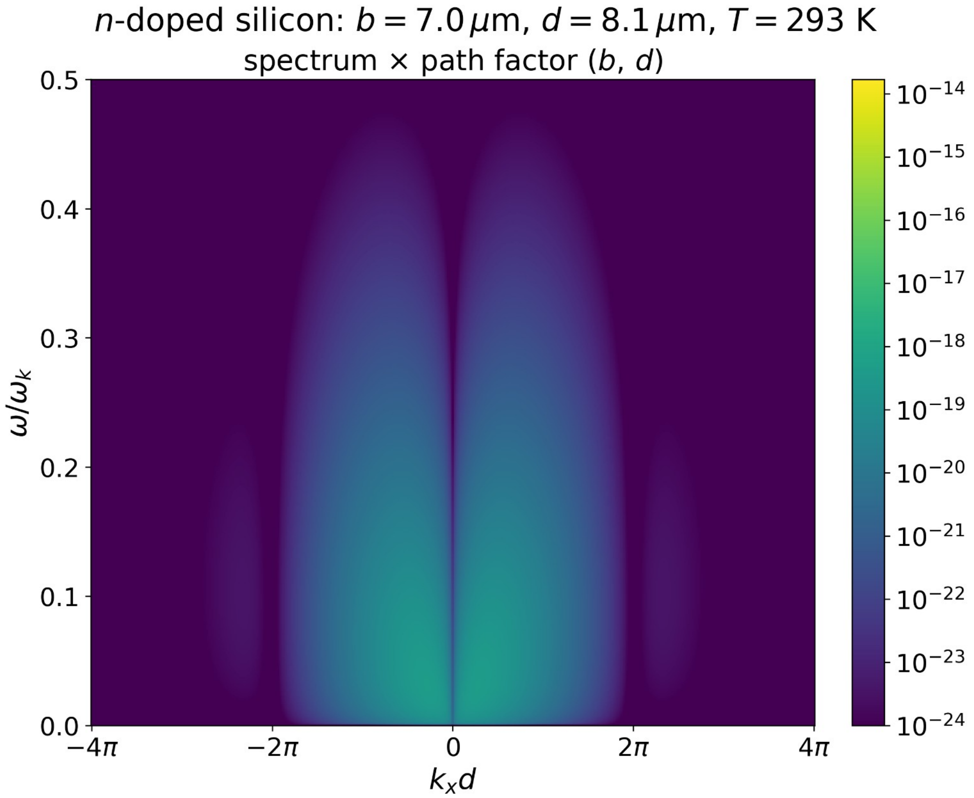

Elements of “Weighted EELS” Model

$$\gamma(b, d, T) = \int_0^\infty \mathrm{d}\omega \int_{-\infty}^{\infty} \mathrm{d}k_x \frac{\mathrm{d}^3 P}{\mathrm{d}\omega\, \mathrm{d}k_x\, \mathrm{d}z} \left[1 - \cos(k_x d)\right] \coth\left(\frac{\hbar\omega}{2k_B T}\right)$$

- This decomposition allows us to clearly see where *b*, *d*, and *T* each contribute

$$\mathcal{V} = \exp\left[-\gamma(b, d, T) L\right]$$

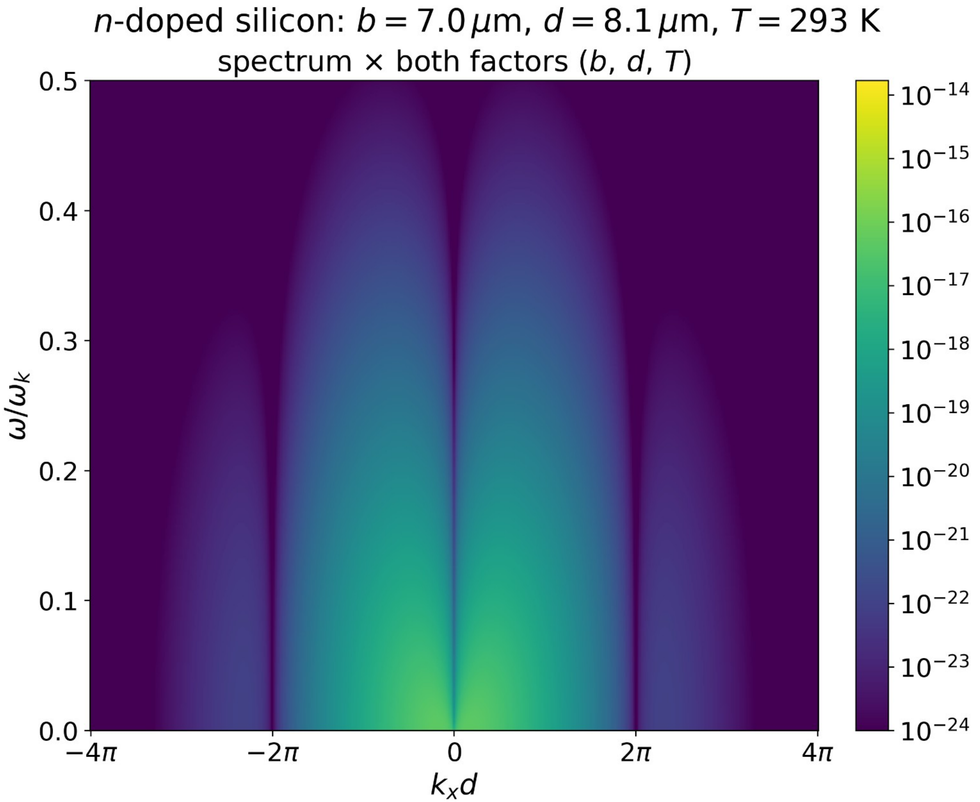

Isolating Contributions

- We can also use less sophisticated EELS loss models

$$\gamma(b,d,T) = \int_0^\infty \mathrm{d}\omega \int_{-\infty}^{\infty} \mathrm{d}k_x \, \frac{\mathrm{d}^3 P}{\mathrm{d}\omega\, \mathrm{d}k_x\, \mathrm{d}z} \left[1 - \cos(k_x d)\right] \coth\left(\frac{\hbar\omega}{2k_B T}\right)$$

- This lets us isolate contributions to observations

$$\mathcal{V} = \exp\left[-\gamma(b,d,T)L\right]$$

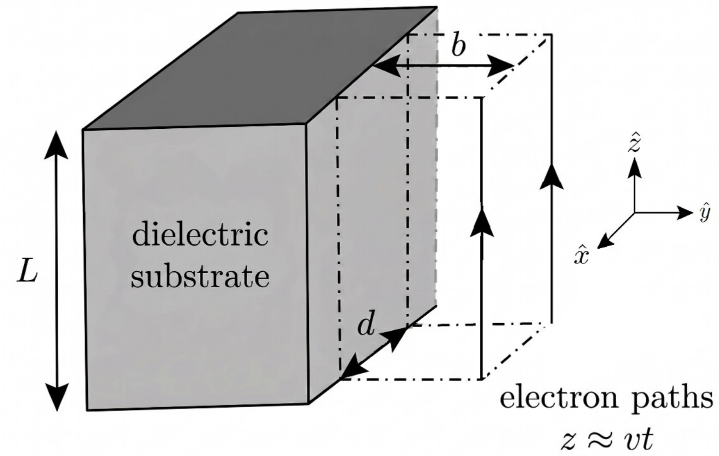

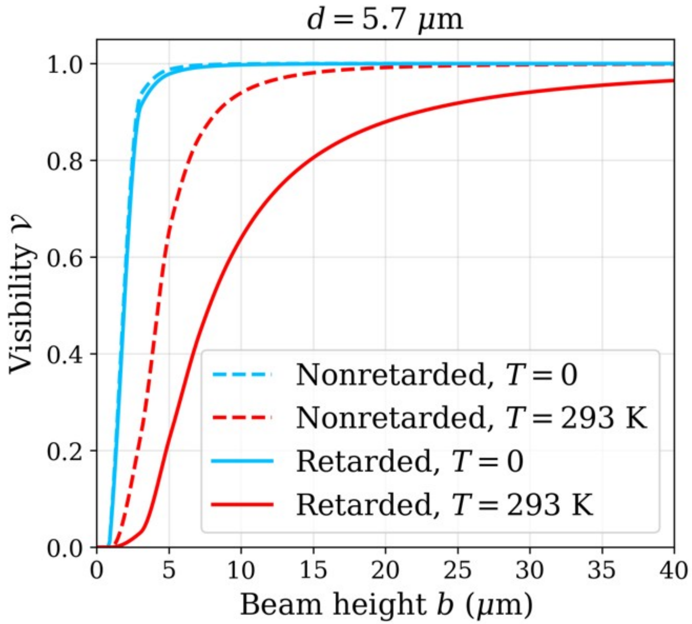

n-doped silicon

Future Experiments

- This model lets us consider how *V* varies with *T*

$$\gamma(b,d,T) = \int_0^\infty \mathrm{d}\omega \int_{-\infty}^{\infty} \mathrm{d}k_x \, \frac{\mathrm{d}^3 P}{\mathrm{d}\omega\, \mathrm{d}k_x\, \mathrm{d}z} \left[1 - \cos(k_x d)\right] \coth\left(\frac{\hbar\omega}{2k_B T}\right)$$

- Visibility declines sharply with increasing *T*

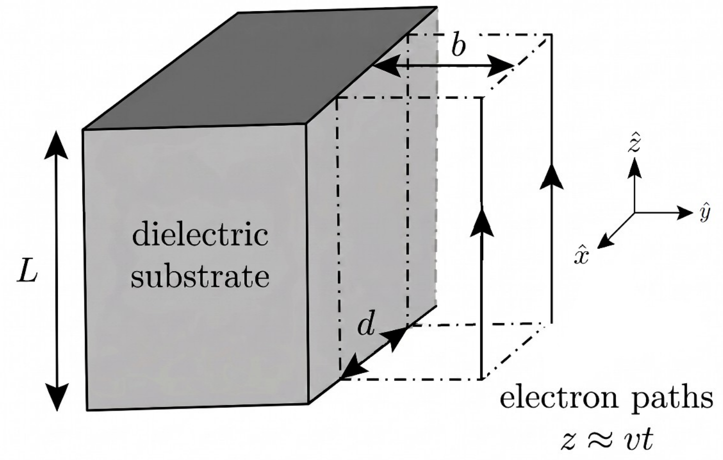

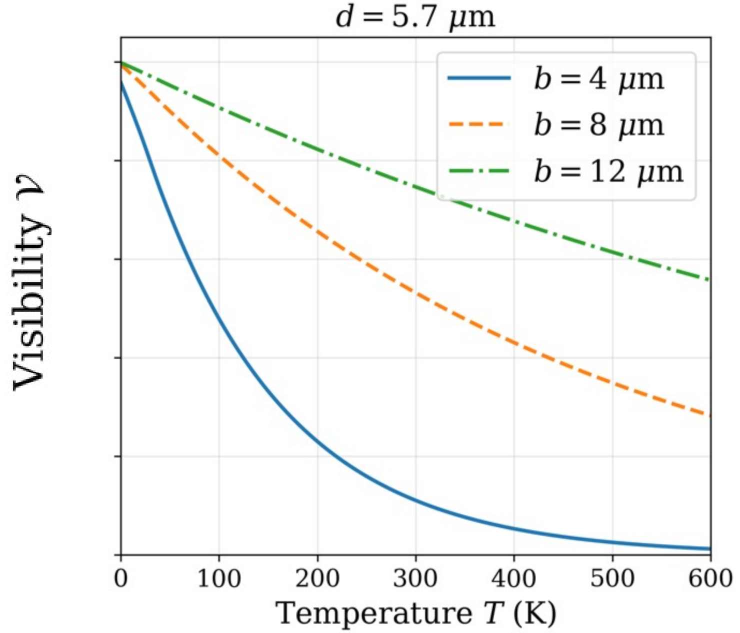

n-doped silicon

Further Modeling

- Velasco *et al.* have suggested a generalized result for the visibility that encourages numerical calculations

$$P(\mathbf{r},\mathbf{r}') = \int_0^\infty d\omega \left[n_T(\omega) + \frac{1}{2}\right] [\Gamma(\mathbf{r},\mathbf{r},\omega) + \Gamma(\mathbf{r}',\mathbf{r}',\omega) - 2\,\Gamma(\mathbf{r},\mathbf{r}',\omega)]$$

$$\Gamma(\mathbf{r},\mathbf{r}',\omega) = \frac{4e^2}{\hbar} \int_{-\infty}^{\infty} dz'' \int_{-\infty}^{\infty} dz''' \cos\left[\frac{\omega}{v}(z - z' - z'' + z''')\right] \mathrm{Im}\{-G_{zz}(\mathbf{R}, z'', \mathbf{R}', z''', \omega)\}$$

- For the half-plane geometry, this is equivalent to the formalism we have discussed here today

Free-electron decoherence: Theory and applications

Cruz I. Velasco, Valerio Di Giulio, F. Javier García de Abajo arXiv:2602.14693

Conclusion

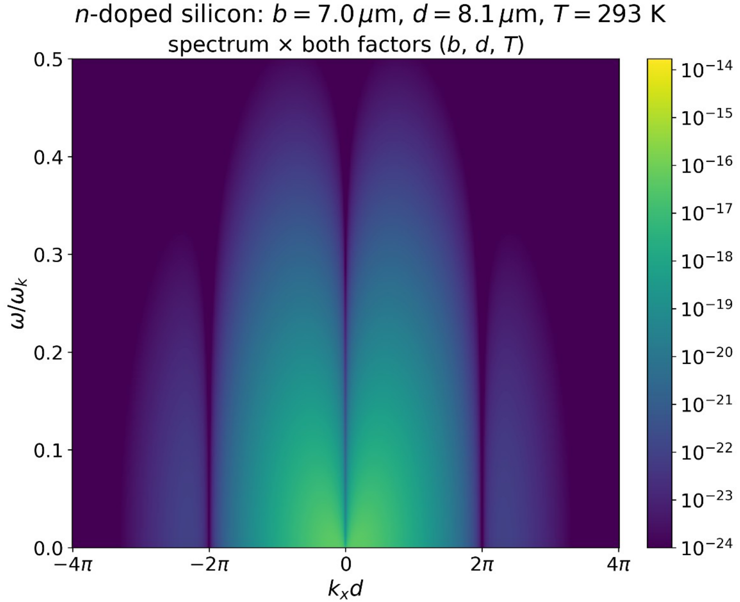

- Fringe decoherence is determined by mode-resolved EEL probabilities
- Channels are weighted by how they distinguish electron paths
- Temperature dependence in fringe visibility should be measurable

$$\mathcal{V} = \exp\left[-\gamma(b,d,T)L\right]$$

$$\gamma(b,d,T) = \int_0^\infty \mathrm{d}\omega \int_{-\infty}^{\infty} \mathrm{d}k_x \, \frac{\mathrm{d}^3 P}{\mathrm{d}\omega\,\mathrm{d}k_x\,\mathrm{d}z}\left[1-\cos(k_x d)\right]\coth\left(\frac{\hbar\omega}{2k_B T}\right)$$

Surface Excitations, Energy Loss, and Decoherence in Electron Interferometry

David Kordahl

arXiv:2606.01004v2